Numerical Simulation of Separating Discharge in the Belt Transfer System

Masami Kadonaga, Tomomi Katoh, Tomoko Takahashi, and Yumiko Kishi
Ricoh Co. Ltd., Yokohama, Japan

The belt transfer system is one of the image transfer processes used in electrophotography. In this process, paper clings to the electro-resistive belt, and is stably fed through the processor. However, electrical discharge may occur between the paper and the belt when the paper is separated from the belt under particular conditions. This discharge is named "separating discharge". Because this discharge causes image degradation, it is important to make clear the separating discharge phenomenon. A model experiment and numerical simulation of separating discharge are carried out for the study of such phenomena. When the sheet is charged at low electrification level, local strong discharge occurs intermittently. On the other hand, the separating discharge becomes continuous and weak when the sheet is charged at high electrification level. Toner movement due to the discharge is also numerically simulated using discrete element method, and the result shows that the image degradation occurs at low electrification level of the sheet, whereas it does not occur at high electrification.

Journal of Imaging Science and Technology 45: 547–555 (2001)

Introduction

The belt transfer system is one of the image transfer processes used in electrophotography.[1,2] In this process, paper clings to the electro-resistive belt, and is stably fed through the processor. However, electrical discharge may occur between the paper and the belt when the paper is separated from the belt under particular conditions. This discharge is named "separating discharge". Because this discharge causes image degradation, it is important to make clear the separating discharge phenomenon. A model experiment is carried out in order to construct a simulating model of this separating discharge and image degradation. A model that explains the generation of separating discharge patterns and image degradation is proposed, and numerical simulation based on this model is carried out.

The Belt Transfer System

The schematic diagram of the belt transfer system is shown in Fig. 1. The paper is held on the electro-resistive belt and fed under the photoconductor. This system assures stable and fast feeding for various kinds of paper. Toner is transferred from the photoconductor to the paper at the nip in the transfer region. Because the electric field strength for the transfer is large in the vicinity of the nip, a weak discharge occurs between the paper and the photoconductor, and charges the paper with the same polarity as the toner. Under normal condition, the charge on the paper flows away through the paper and the belt. When the temperature and the humidity are low, the paper resistance is so high that the charge remains on the paper. Thus discharge between the paper and the belt may occur when the charged paper is separated from the belt. This discharge, named "separating discharge", may degrade the image that has not yet been fixed on the paper.

Objective

The objective is to simulate the image degradation due to separating discharge between the paper and the transfer belt using the model based on the experiment, so as to make a suggestion for preventing the image degradation in the belt transfer system.

Model Experiment

In order to investigate the phenomena of the separating discharge, a model experimental setup is constructed.[3] The schematic diagram of the experimental setup and pictures of it are shown in Fig. 2 and Fig. 3 respectively. A PET [poly(ethylene terephthalete)] sheet

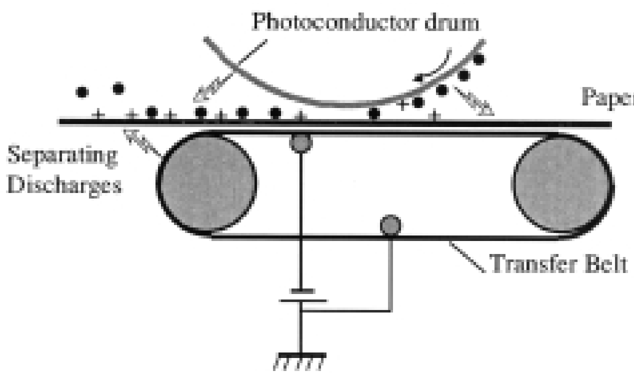

Figure 1. The schematic diagram of the belt transfer system.

Original manuscript received January 23, 2001

Previously presented at IS&T's NIP16: International Conference on Digital Printing Technologies, October 15-20, 2000, Vancouver, B.C. Canada.

©2001, IS&T—The Society for Imaging Science and Technology

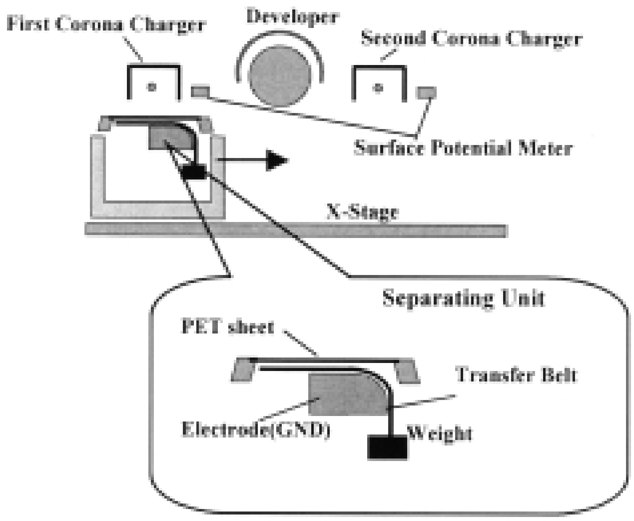

Figure 2. Schematic diagram of the experimental setup.

of 100 μm thickness is used instead of paper because of its high and stable resistance. The unit called "separating unit", consists of the PET sheet, transfer belt, electrode and weight, as shown in Fig. 2. A transfer belt is set under the PET sheet. This PET sheet is cleaned with alcohol beforehand for the elimination of dust and charge on the surface. The weight (200 g) is hung at the end of the transfer belt to make tension and separation easy. The backside of the belt is connected to the grounded electrode. The belt consists of two layers: surface layer (thickness 15 μm) made of Teflon and main layer (thickness 500 μm) made of chloroprene rubber. The volume resistivity of the belt is 7.22×10^7 ohm-m. Figure 4 shows the sequence of the experiment schematically. The first step of the experiment is charging the sheet by a corona charger as shown in Fig. 4(a). The surface potential of the sheet after the first charging is 150 V in positive electrification and –150 V in negative electrification. This charging corresponds to the discharge between the OPC and the paper in the inlet of the transfer region in a real photocopier. The second process of the experiment is development of the sheet by the developer and charging again by the second corona charger (Fig. 4(b)). The development parameters are adjusted in order to obtain half the toner image on the sheet, because image degradation can be recognized easily under these conditions. Positive toner is used when the sheet is positively charged, and *vice–versa*. This corresponds to the toner transfer from the photoconductor to the paper in a real photocopier. The polarity of the second charging is the same as that of the first charging. This charging by the second corona corresponds to the discharge in the outlet of the transfer region in a real photocopier, and this charging can modify the surface potential of the sheet before separation. The last process of the experiment is to slide the electrode and to separate the belt from the sheet (Fig. 4(c)). The sliding speed is 2.5 mm/s and the sliding distance is 30 mm. This last process corresponds to the separation of the paper from the belt in a real photocopier. The experiments are carried out under the environmental conditions of 20°C and 10% RH.

Experimental Results

When the electrode is slid after forming the image on the sheet, image degradation can be observed with the movement of the electrode. Figure 5(a) shows the example of the image degradation when the surface potential before separation (Vs) is + 240 V. This image degradation seems to be created by the separating discharge between the sheet and the belt. The discharge pattern of the opposite side of that sheet is shown in Fig. 5(b), which is obtained by cascade development[4] with positively charged toner. The shape of the degraded image on the surface side of the PET sheet is in good correspondence with the discharge pattern on the backside of the sheet. In order to confirm that the image degradation is due to separating discharge between the sheet and the belt, discharge observation is carried out. Figure 6 shows the schematic diagram of the observation. As the transparent PET sheet without toner development is used, discharge light can be observed through two cascaded image intensifiers in a darkroom. An example of the observed light from the viewpoint above the sheet is shown in Fig. 7. The shape of the discharge light resembles with that of the discharge pattern shown in Fig. 5. From these results, image degradation should be due to the separating discharge between the sheet and the belt. Figure 8 shows

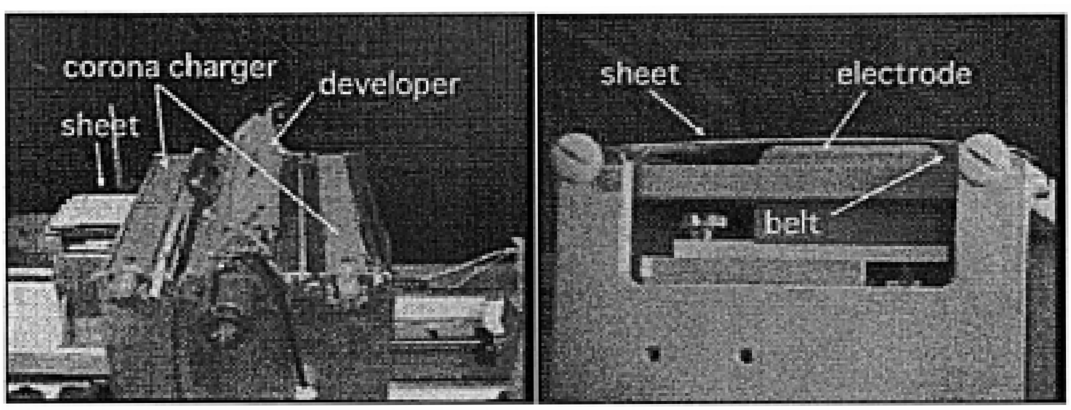

(a) Experimental setup.

(b)Magnified view of the separating unit.

Figure 3. Pictures of the experimental setup.

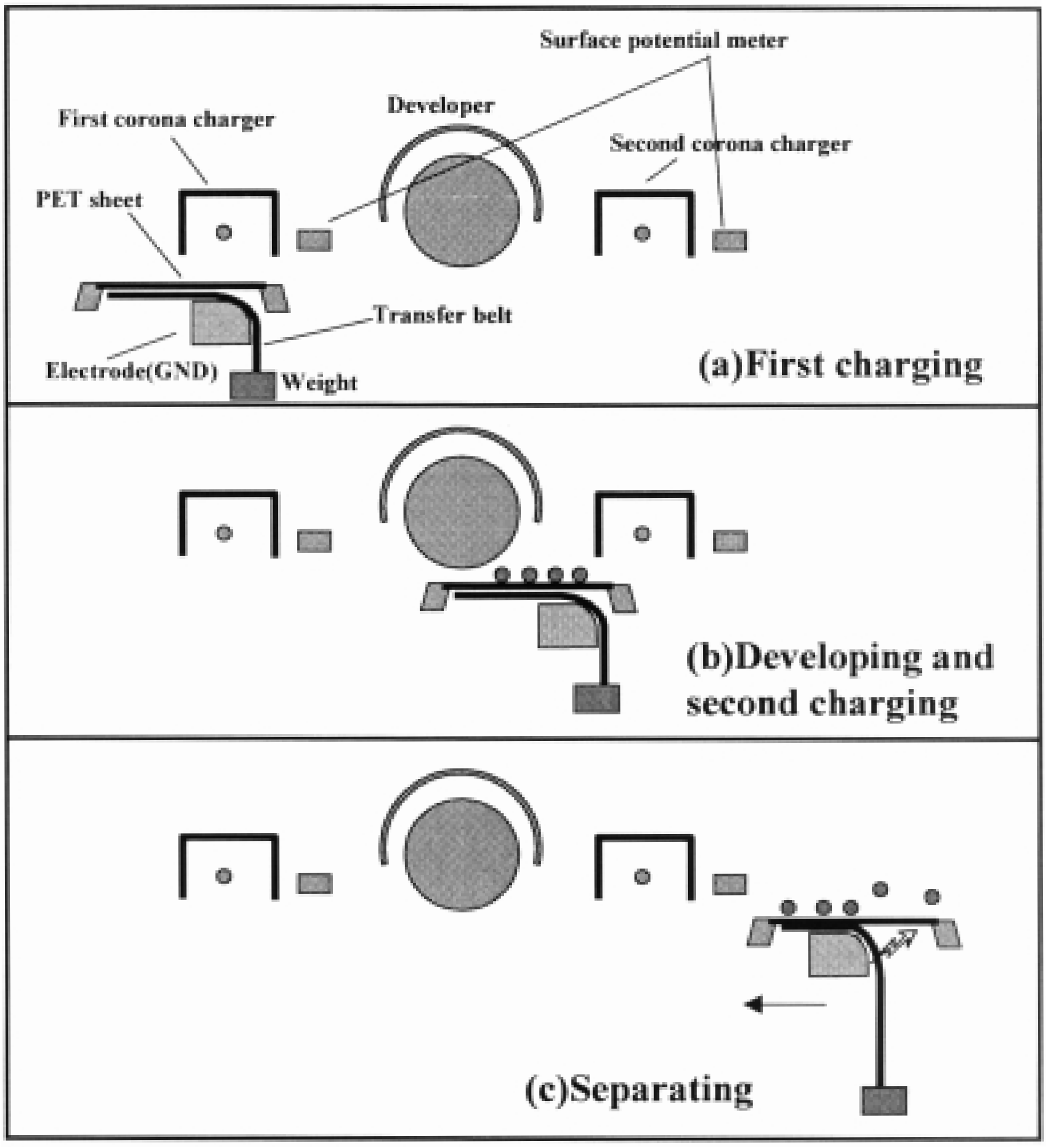

Figure 4. The sequence of the experiment.

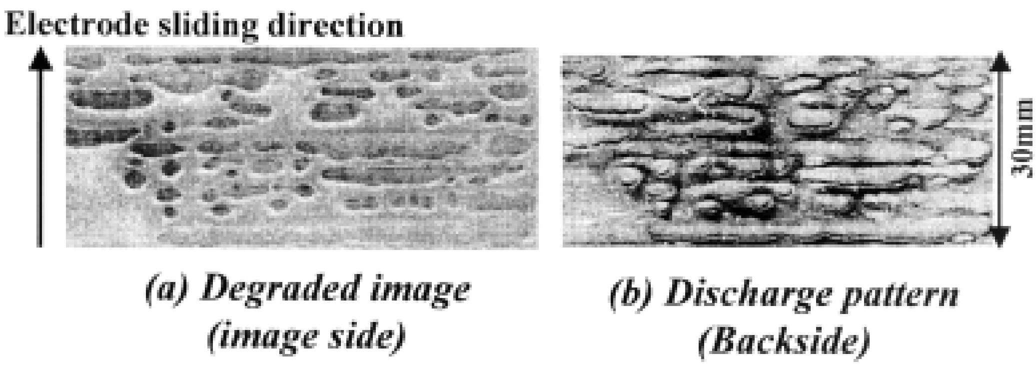

Figure 5. Agreement between degraded image and discharge pattern (*Vs* = + 240 V).

the discharge pattern and observed light emission when the sheet is negatively charged before separation. The completely different shapes are observed from Fig. 5(b) and Fig. 7. When the sheet is positively charged, the shapes of the discharge pattern and discharge light are round shapes. On the other hand, when the sheet is negatively charged the shape of the discharge pattern and the discharge light are tree-like shapes. The effect of the polarity on the discharge patterns is very similar to that on Lichtenberg's figures, which are well known as surface discharge patterns. The surface discharge may be involved with the generation of discharge patterns.

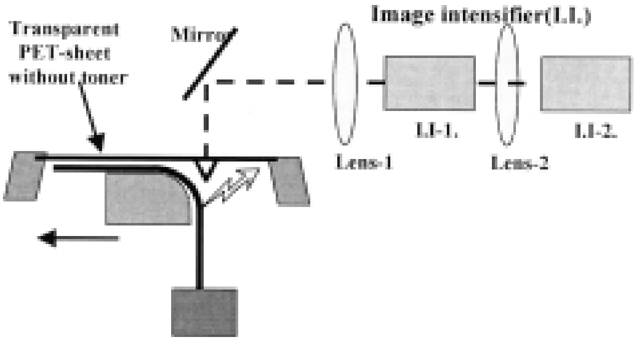

Figure 6. Experimental setup for the observation of light emission due to separating discharge.

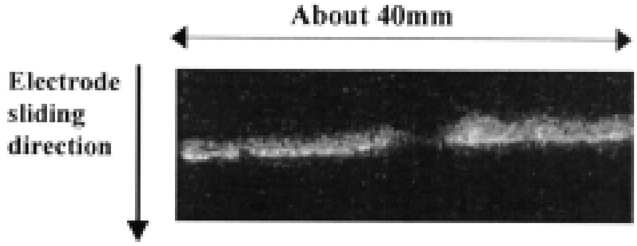

Figure 7. Light emission of the separating discharge (Vs = 240 V).

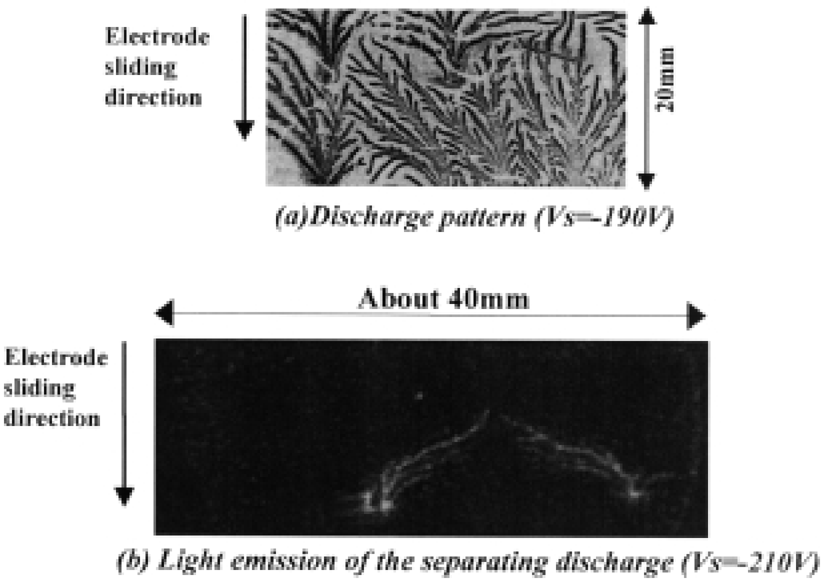

Figure 8. Experimental results when the sheet is negatively charged.

Model of Generating Image Degradation

A generating model for image degradation is proposed on the basis of examination of experimental results. Figure 9 shows the time sequence of the model near the discharge point between the PET sheet and the belt. When the separation between the charged sheet and the belt begins, induced charge appears on the backside of the sheet facing the belt. As the separation proceeds, the potential at a point on the surface rises, and a separating discharge occurs when Pashen's breakdown condition is fulfilled. The discharge gap is so large that a strong discharge may occur, and a large amount of charge may move due to abnormal discharge (Fig. 9(a)). The electric field strength of the discharge point on the PET sheet is so high that the surface discharge also takes place and creates a discharge pattern on the backside of the sheet (Fig. 9(b)). The arrows express the flows of the charge due to the surface discharge on the backside of the sheet. Toners deposited on the PET sheet move according to the electric field around the discharge point and the image degradation is generated (Fig. 9(c)). Because the PET sheet at that point is neutralized and the potential across the gap becomes less than the threshold voltage, subsequent discharge can not take place for a while. As the sheet moves more, and the charged part is far enough from the discharge point, the potential across the gap increases again and the next discharge takes place (Fig. 9(d)). Thus one cycle of the discharge and toner movement is completed and the process repeats itself forming periodic patterns.

Simulation Model

In order to certify this new model, 2-dimensional simulation of the separating discharge with toner movement is carried out according to the following steps.

Step 1:

Calculation of the Electric Field to obtain the potential distribution around the PET sheet and the belt at time T. The thickness of the belt is ignored in this simulation because the separating speed (2.5 mm/s) is enough slow to treat the belt as a conductor. A Boundary Fitting Coordinate Mesh is used to fit the belt shape. Poisson's equation is solved by the finite difference method taking into consideration the movement of the PET sheet.

Step 2:

Calculation of the Abnormal Discharge between the sheet and the belt. Using Paschen's law for the break-

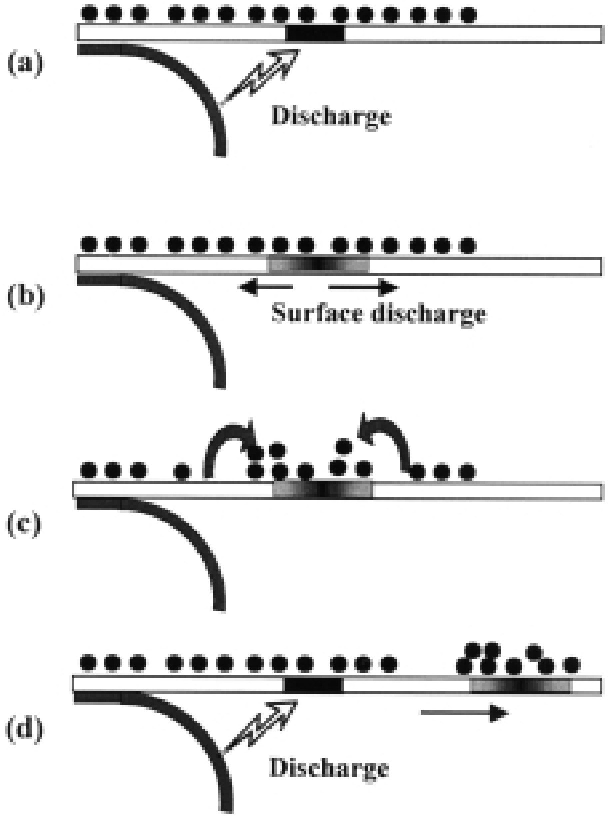

Figure 9. Generating model of image degradation.

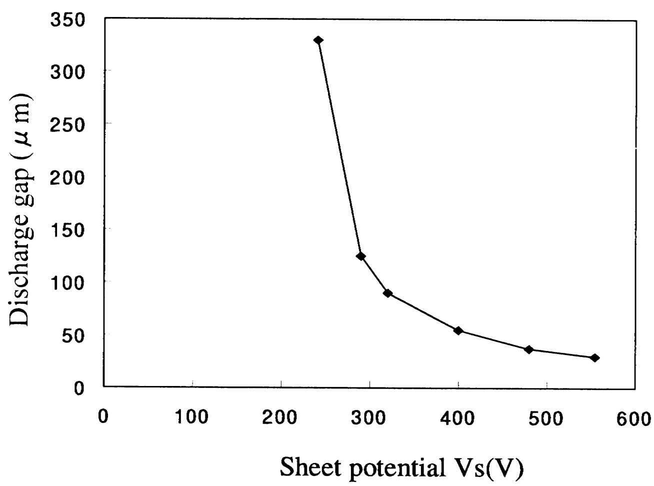

Figure 10. Relation between discharge gap and *Vs*.

down voltage, the discharge gap can be derived as shown in Fig. 10. When the discharge occurs at the gap $g(m)$, the amount of charge dQ (C/m^2), deposited on the sheet is estimated from the experimental result. Here, the discharge density is defined as the number of discharges in 30 mm along the separating direction. The relation between the discharge density and Vs is shown in Fig. 11, and the relation between the surface potential of the backside of the sheet and Vs is shown in Fig. 12. From these three relations, the amount of charge from one abnormal discharge can be estimated, and is shown in Fig. 13. The fitting curve is expressed by Eq. 1.

$$dQ = -0.002 \times \ln(g) - 0.0226 \quad (1)$$

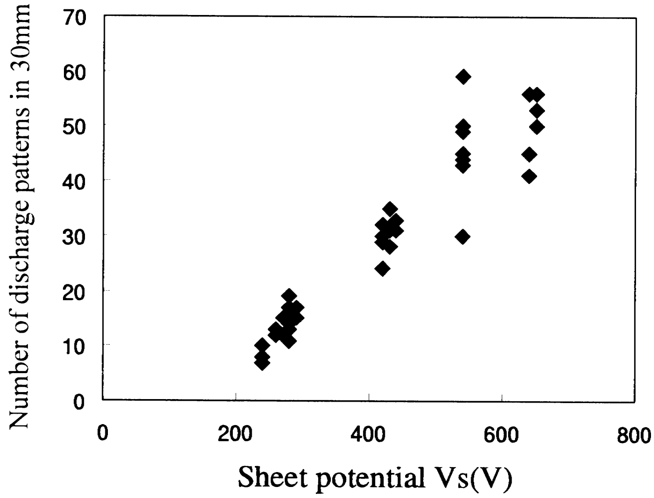

Figure 11. Relation between discharge density and *Vs*.

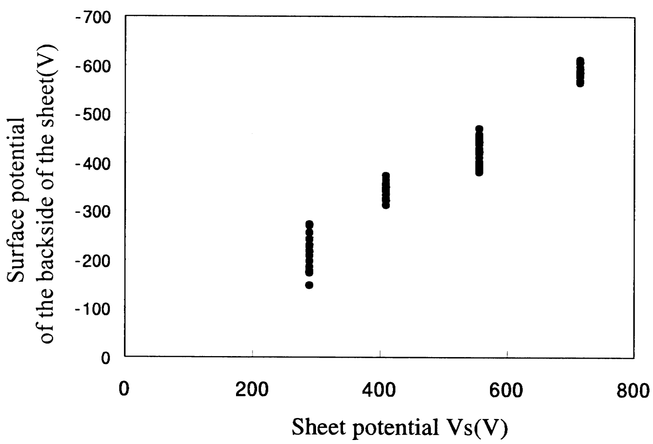

Figure 12. Relation between backside potential of the sheet and *Vs*.

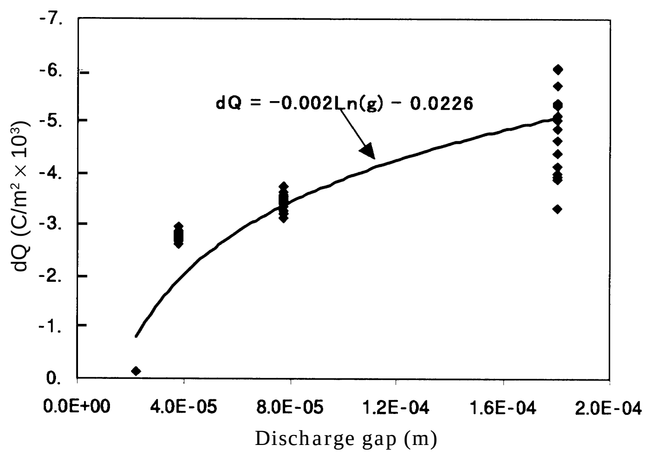

Figure 13. Discharge amount from one discharge.

Step 3:

Calculation of the Surface Discharge. The electric field after the abnormal discharge is recalculated because discharge disturbs the electric field. Next, the electric field strength E is estimated at every point on the sheet. If the electric field strength is higher than the breakdown field strength of the surface discharge (Elim), surface discharge may take place and charge, dq (C), is forced to move in the direction according to the electric field around the point. The amount of charge dq is supposed to be proportional to the electric field as is shown in Eq. 2.

$$dq = \alpha \times E \text{ (in case of } E > E\text{lim)} \tag{2}$$

where α is the parameter for calculation of the surface discharge which acts like electric conductivity. Elim = 3×10^6 V/m and $\alpha = 3 \times 10^{-14}$ Cm/V are used in this study. Both parameters are adopted in order to simulate the experimental results. The value of α is not so important, because Step 3 should be repeated until surface discharge does not occur at any point on the PET sheet. The charge distribution on the PET sheet after Step 3 is approximately same when the value of α is sufficiently small. After Step 3, the electric field at time T is obtained.

TABLE I. Calculation Parameters

Surface potential of the belt	0 V
Thickness of the belt	0 µm
Separating curvature	R20 mm
Sheet thickness	100 µm
relative dielectric constant of the sheet	3
Sheet velocity	2.5 mm/s
Number of mesh in x direction	320
Number of mesh in y direction	55
(air above sheet)	(25)
(sheet)	(10)
(air gap)	(20)
Time step dt	100 µs
Boundary conditions	
Top, Right, Left	Symmetrical boundary
Bottom (Belt surface)	0 V

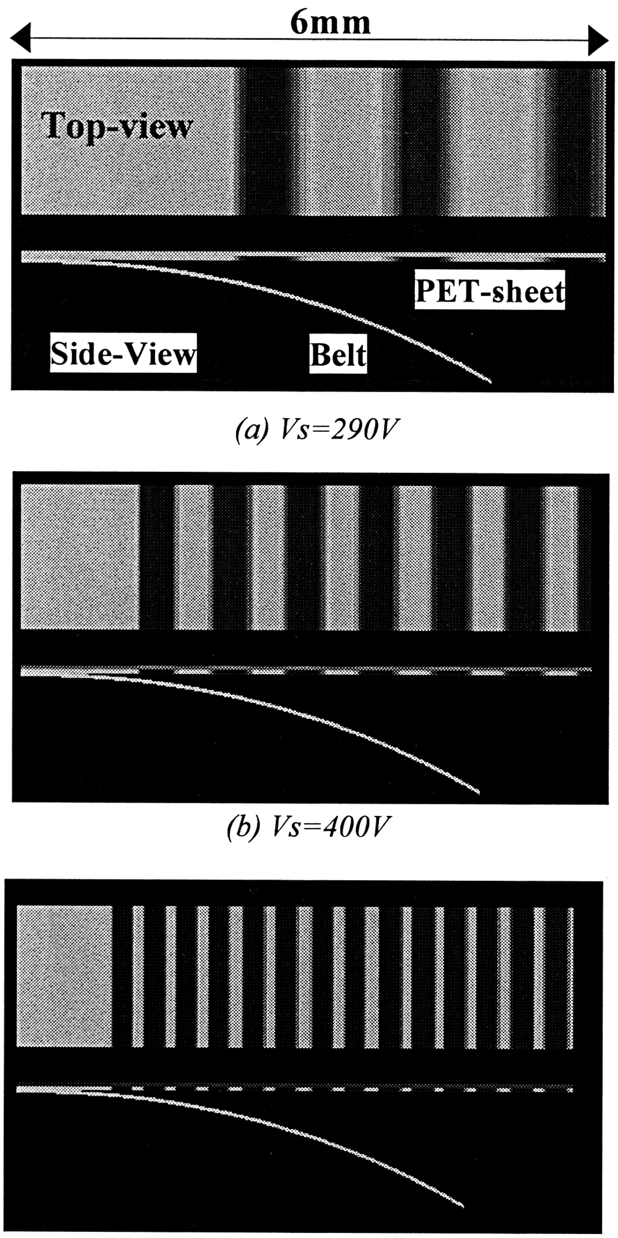

Figure 14. The separating discharge patterns for various surface potential obtained by simulation.

Step 4:

Calculation of the Toner Movement. Force and movement of toner are calculated using the discrete element method.[7] The total force on toner $F(T)$ is sum of each forces such as force due to electric field (Fe), forces due to other charged toners (Fq), forces due to adhesion force (Fa), and forces due to air resistance (Fr), as is shown in Eq. 3. The velocity and position of the toner can be calculated using Eqs. 4 and 5.

$$F(T) = ma = Fe + Fq + Fa + Fr \tag{3}$$

Fe : force due to electric field (qE)
Fq : force due to other charged toners
Fa : force due to adhesion force while toner is on the sheet
Fr : force due to air resistance while flying

$$v(T + dt) = v(T) + (F(T)/m)dt \tag{4}$$

$$x(T + dt) = x(T) + v(T)dt + 0.5(F(T)/m)dt^2 \tag{5}$$

m : weight of toner
q : charge of toner
v : velocity of toner
x : position of toner
F : force on toner
dt : time step of the calculation

Step 5:

Time is Advanced ($T = T + dt$). The PET sheet moves forward, and then Step 1 is repeated, etc.

Simulation Results

Surface Discharge Pattern

In order to confirm the separating discharge model, numerical simulation without toner movement is carried out and is compared with the experiment. Calculation conditions are shown in Table I. The results are shown

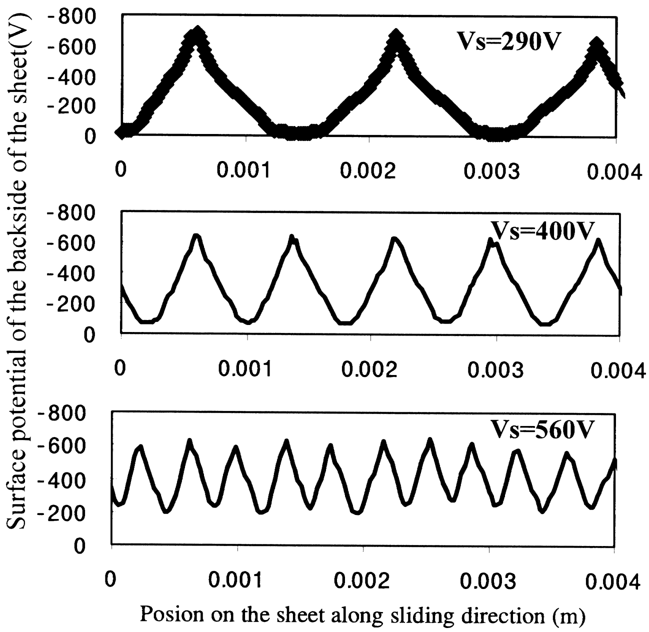

Figure 15. The potential distribution on the PET sheet obtained by simulation.

in Fig. 14, indicating the charge distribution on the backside of the PET sheet in gray scale. "Top-view" shows the charge distribution on the backside of the sheet. The dark parts indicate highly charged regions. Figure 14(a) is the case for Vs = 290 V, (b) is Vs = 400 V, and (c) is Vs = 560 V. Periodic charging patterns can be recognized on the PET sheet. Figure 15 is the simulation result showing a series of charge distribution on the PET sheet for various surface potentials corresponding to Fig. 14. As the surface potential before separation increases, amount of charge deposited on the backside of the sheet decreases because of reduction of the discharge gap. The excess value of the electric field over Elim in Step 3, namely (E – Elim), decreases, and charge, dQ, estimated from Eq. 2 also decreases. Hence, width of the discharge pattern becomes small due to smaller amount of charge, which is forced to move by surface discharge. The next discharge happens easily due to smaller distortion of the potential from smaller discharge pattern, and the period of the pattern becomes smaller. Figure 16 shows the experimental results of the discharge pattern obtained by cascade development on the backside of the sheet. As the dependence of the size and period of the discharge pattern on the surface potential Vs is the same as the simulation result. The potential distribution along the electrode sliding direction measured at every 32 μm using the high resolution surface potential meter[8] is shown in Fig. 17. The agreement of the numerical simulation with the experiment for the separating discharge phenomena is excellent.

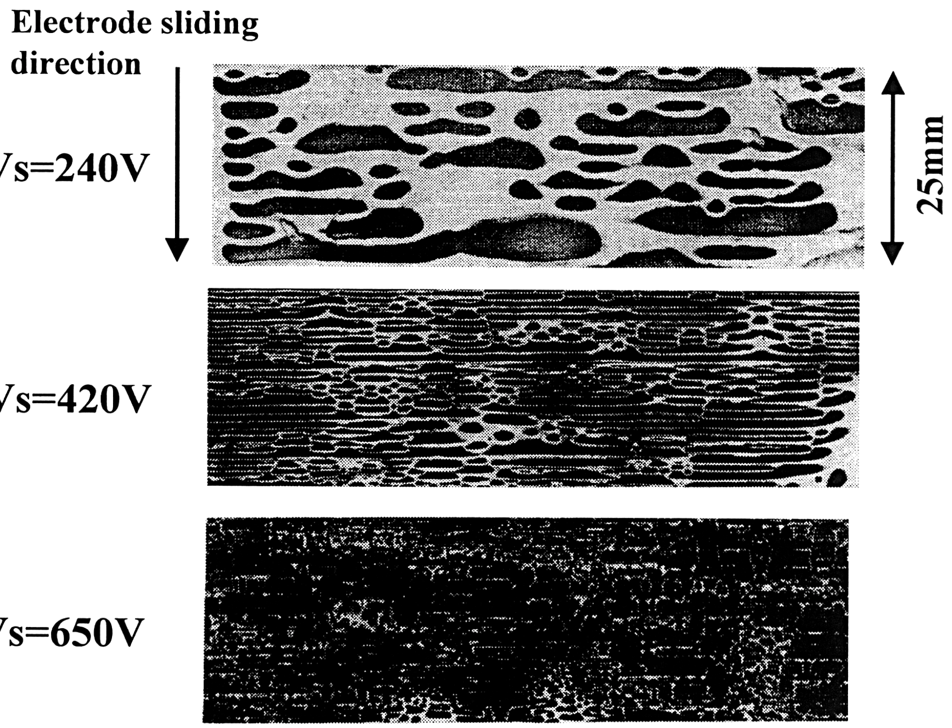

Figure 16. The separating discharge patterns for various surface potentials obtained by experiment.

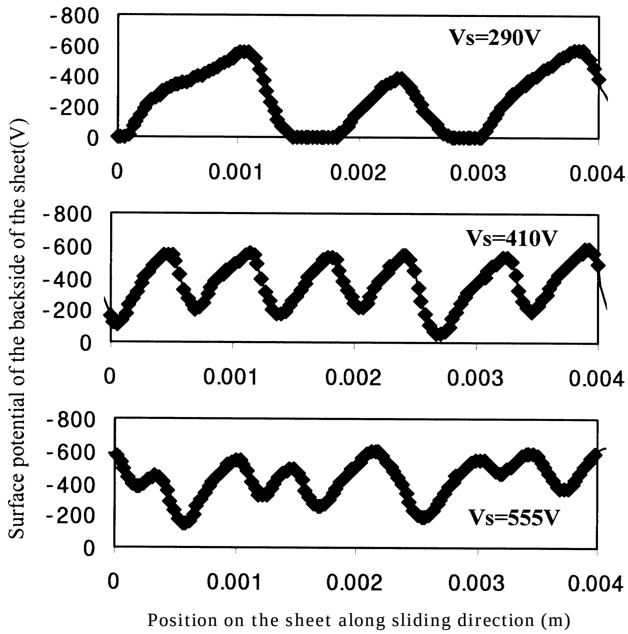

Figure 17. The potential distribution on the PET sheet obtained by experiment.

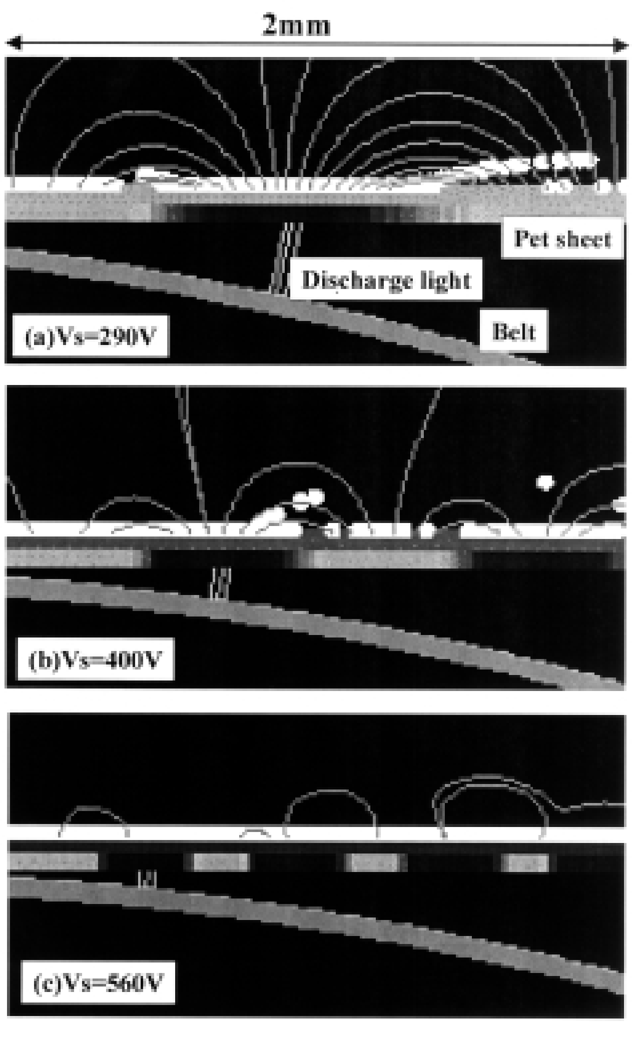

Figure 18. The simulation result with the toner movement.

TABLE II. Calculation Parameters

Adhesion force between toner and sheet	7 nN
Toner diameter	7 μm
Toner q/m	20 μC/g
Time step dt	1.0 μs

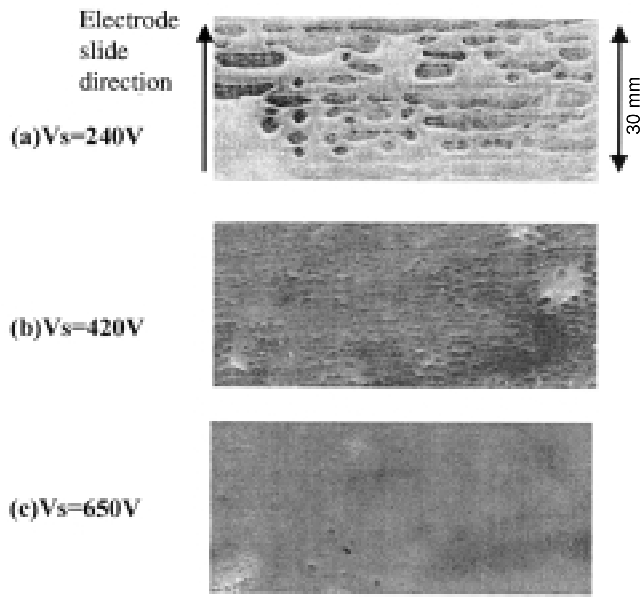

Figure 19. The experimental results of image degradation.

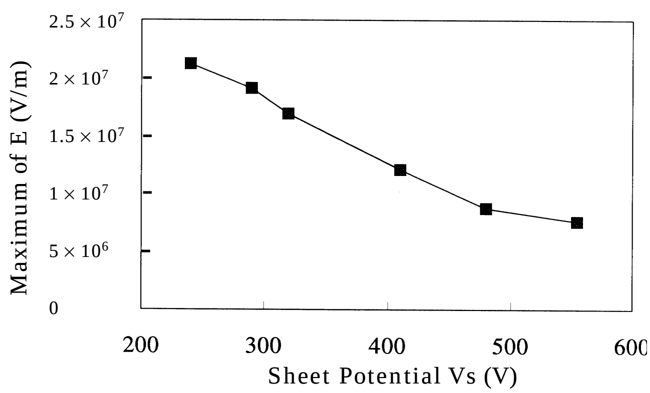

Figure 20. The relation between the electric field strength and surface potential *Vs*.

Image Degradation

The simulation result with toner movement due to discharge is shown in Fig. 18. Calculation parameters are shown in Table II. The adhesion force between toner and sheet is adopted in order to simulate the experimental results. The value of this force (7 nN) seems to be small in comparison with usual values. In this case, toners, which have positive charge, are deposited on the positively charged sheet and the Coulombic force reduces the adhesion force. In Fig. 18, toner is shown in white and its diameter is magnified 5 times for easy recognition. Lines of electric force are also shown as white lines. In the initial condition, toners are deposited uniformly on the PET sheet. When the surface potential before separation is 290 V and 400 V, toners are forced to move towards the discharge point due to the electric field created by discharge, and image degradation occurs (Figs. 18(a) and 18(b)). On the other hand, image degradation does not occur even though the separating discharge actually happens when the surface potential is 560 V (Fig. 18(c)). Experimental results of image degradation are shown in Fig. 19. When the surface potential before separation is 650 V, image degradation does not occur. From these results, it is confirmed that image degradation can be suppressed when the sheet is charged at a high electrification level.

Figure 20 shows the relation between the maximum value of the electric field strength on the sheet after the separation and surface potential before separation. As the surface potential increases, the electric field strength decreases. In case of the adequately charged sheet, as the separating discharge tends to occur in a small gap, the discharge becomes weak according to Eq. 1. Hence size and period of the pattern on the backside of the sheet becomes small as is shown in Fig. 14, and the electric field strength on the sheet becomes too small to detach toner from the sheet. Therefore, image degradation can be suppressed when the sheet is sufficiently charged. In order to suppress the image degradation due to separating discharge, two proposals are inferred from these results. One is to suppress the separating discharge with a charge-neutralized sheet. The other is to make sheet sufficiently charged before separation so as to make the discharge weak and to restrain toner movements.

Conclusion

It is confirmed from the model experiment that the image degradation in the belt transfer system is due to the separating discharge between the paper and the belt. Separating discharge patterns are simulated numerically, and the simulation results show good agreement with experiments. Toner movement due to discharge is also simulated using the discrete element method, and the result shows that image degradation occurs at low electrification level of the sheet, whereas it does not occur at high electrification level. In the belt transfer system, charging the paper at a high electrification level before separation realizes excellent image transfer without image degradation.

Acknowledgment. The authors are grateful to Professor Yuzo Takahashi of Tokyo University of Agriculture and Technology for his valuable discussion and advice on the separating discharge.

References

1. Y. Harasawa, I. Matsuda, S. Takano, H. Yu, Y. Kawaishi, H. Kamiyama, T. Motohashi, M. Takahashi, and T. Bisaiji, U.S. Patent, 5,461,461 (1995).
2. I. Matsuda, S. Takano and Y. Harasawa, U.S. Patent, 5,495,317 (1996).
3. T. Katoh, M. Kadonaga and T. Takahashi, *Proc. of IS&T's NIP12*,IS&T, Springfield, VA, 1996, p. 370.
4. R. M. Schaffert, *Electrophotography*, Focal Press, London, 1975.
5. F. H. Merrill and A. von Hippel, *J. Appl. Phys.* **10,** 873 (1939).
6. M. Kadonaga, T. Katoh and T. Takahashi, *J. Imaging Sci. Technol.* **43**(3), 274 (1999).
7. P.A. Cundall and O.D.L.Strack, *Geotechnique* **29**, 47 (1979).
8. J. Takahashi and T. Katoh, *Trans. IEE Japan* **117-E**(12), 594 (1997).